Saudi Pharmaceutical Journal 28 (2020) 495–503

Contents lists available at ScienceDirect

Saudi Pharmaceutical Journal

journal homepage: www.sciencedirect.com

Original article

Anticancer activity of THMPP: Downregulation of PI3K/ S6K1 in breast cancer cell line

Suresh Palanivel [a,b], Akshaya Murugesan [a,b,c], Olli Yli-Harja [b,d,e], Meenakshisundaram Kandhavelu [a,b,*]

[a] Molecular Signaling Lab, Faculty of Medicine and Health Technology, Tampere University and BioMediTech, Tays Cancer Center, Tampere University Hospital, P.O. Box 553, 33101 Tampere, Finland

[b] Institute of Biosciences and Medical Technology, 33101 Tampere, Finland

[c] Department of Biotechnology, Lady Doak College, Thallakulam, Madurai 625002, India

[d] Computaional Systems Biology Group, Faculty of Medicine and Health Technology, Tampere University and BioMediTech, Tays Cancer Center, Tampere University Hospital, P.O. Box 553, 33101 Tampere, Finland

[e] Institute for Systems Biology, 1441N 34th Street, Seattle, WA 98103-8904, USA

ARTICLE INFO

Article history:
Received 15 January 2020
Accepted 29 February 2020
Available online 19 March 2020

Keywords:
Tetrahydroquinoline
Apoptosis
Gene expression
EGFR
Docking
ADME
QSAR

ABSTRACT

Breast cancer is the most common cancer that majorly affects female. The present study is focused on exploring the potential anticancer activity of 2-((1, 2, 3, 4-Tetrahydroquinolin-1-yl) (4 methoxyphenyl) methyl) phenol (THMPP), against human breast cancer. The mechanism of action, activation of specific signaling pathways, structural activity relationship and drug-likeness properties of THMPP remains elusive. Cell proliferation and viability assay, caspase enzyme activity, DNA fragmentation and FITC/Annexin V, AO/EtBr staining, RT-PCR, QSAR and ADME analysis were executed to understand the mode of action of the drug. The effect of THMPP on multiple breast cancer cell lines (MCF-7 and SkBr3), and non-tumorigenic cell line (H9C2) was assessed by MTT assay. THMPP at IC_{50} concentration of 83.23 µM and 113.94 µM, induced cell death in MCF-7 and SkBr3 cells, respectively. Increased level of caspase-3 and -9, fragmentation of DNA, translocation of phosphatidylserine membrane and morphological changes in the cells confirmed the effect of THMPP in inducing the apoptosis. Gene expression analysis has shown that THMPP was able to downregulate the expression of PI3K/S6K1 genes, possibly via EGFR signaling pathway in both the cell lines, MCF-7 and SkBr3. Further, molecular docking also confirms the potential binding of THMPP with EGFR. QSAR and ADME analysis proved THMPP as an effective anti-breast cancer drug, exhibiting important pharmacological properties. Overall, the results suggest that THMPP induced cell death might be regulated by EGFR signaling pathway which augments THMPP being developed as a potential candidate for treating breast cancer.

1. Introduction

Breast cancer is the most challenging type of cancer worldwide. In 2018, about 2.1 million new breast cancer cases have been diagnosed. In over 100 countries, it ranks as the leading causes of cancer death (Bray et al., 2018). Estrogen receptors (ER) are responsible for approximately 70–75% of inter-tumor heterogeneic nature of breast cancer. Estrogens on binding to ER is responsible for the transcription/expression of many growth factors involving cellular proliferation (Sun et al., 2001). Apart from estrogens, there are many non-steroidal growth factors including EGF and IGF1, that can bind to ER and stimulate proliferation via signal transduction pathways like MAPK pathway (Kato et al., 1995). Progesterone receptor (PR) also plays an equal importance in cancer development and progression as ER.

Abbreviations: THMPP, 2-((1, 2, 3, 4-Tetrahydroquinolin-1-yl) (4 methoxyphenyl) methyl) phenol; IC_{50}, The half maximal inhibitory concentration; FITC, Fluorescein isothiocyanate; AO/EtBr, Acridine orange/ethidium bromide; RTPCR, Reverse Transcriptase PCR; QSAR, Quantitative structure activity relationship; ADME-Absorption, Distribution, Metabolism, and Excretion; MCF-7, Michigan Cancer Foundation-7; SkBr3, Sloan–Kettering Cancer Center; EGFR, Epidermal Growth Factor Receptor; ER, Estrogen Receptor; PR, Progesterone Receptor; PI3K, Phosphoinositide 3-kinase; FACS, Fluorescence-activated cell sorting.

* Corresponding author.

E-mail addresses: suresh.palanivel@tuni.fi (S. Palanivel), akshaya.murugesan@tuni.fi (A. Murugesan), olli.yli-harja@tuni.fi (O. Yli-Harja), meenakshisundaram.kandhavelu@tuni.fi (M. Kandhavelu).

Peer review under responsibility of King Saud University.

Production and hosting by Elsevier

https://doi.org/10.1016/j.jsps.2020.02.015
1319-0164/

The treatment regimens followed in ER+/PR+ breast cancer cases are mostly hormonal/endocrine therapy. It is done by blocking the ER, in-turn controlling the growth promoting effects on the cell. Though, it is recognized as an effective treatment for ER+/PR+ patients, most of the patience develops resistance to such therapies. There is a vital need for the novel therapies over the existing hormonal therapies, thereby extending the progression period, eliminating or reducing the resistance and postpone the chemotherapy (Ciruelos Gil, 2014).

In accordance with this, our research group indulges in synthesis of novel small molecule drugs for multiple cancer treatments. One such phenolic derivatives is, 2-((1, 2, 3, 4-Tetrahydroquinolin-1-yl) (4 methoxyphenyl) methyl) phenol (THMPP), found to have good cytotoxicity activity against bone carcinoma cells (Karjalainen et al., 2017). We hypothesize that THMPP might have anticancer activity against breast cancer and hence we wish to explore the mechanism of its action of the compound THMPP against breast cancer cells.

The present study also signifies that THMPP can induce cell death in breast cancer cells via EGFR signaling pathway. The EGFR overexpressed in metastatic breast cancer cells that influences the downstream signaling pathways such as the ERK MAPK, PI3K-AKT, SRC, PLC-γ1-PKC, JNK, and JAK-STAT pathways. The PI3K/AKT/mTOR pathway is the well-known signaling pathway involved in cell proliferation and survival. In tumorigenesis, this signal cascade is continuously activated even in the absence of any growth factors/ligands. Inhibition of this pathway can suppress the tumor growth and eventually benefit the ER+ patient through endocrine therapy (Martelli et al., 2010). Hence, we also propose to investigate the effect of THMPP in the regulation of PI3K signaling pathway genes in combination with computational analysis.

2. Materials and methods

2.1. Cell lines and culture

Human breast adenocarcinoma cell lines, MCF-7, SkBr3; Triple negative breast cancer cells, MDAMB-231; and rat myoblast cells, H9C2, were obtained from NCCS, Pune. All the cell lines used in the study was EGFR (+). Cells were cultured in Dulbecco's Modified Eagle Medium (DMEM), supplemented with 10% Fetal Bovine Serum (FBS), maintained at 37 °C humidified with 5% CO_2 (Vaiyapuri et al., 2015). THMPP (Fig. 1a) was synthesized by our research group as previously described. Untreated cells were used as a negative control with cyclophosphamide, as a positive control (Fig. 1b). The characterization of the chemical compound and the preparation of THMPP was described in the previously established procedure (Doan et al., 2019, 2017). NMR spectroscopic data of the compound was included as the supplementary file (Supplementary file 1).

2.2. Cytotoxicity assay

The cytotoxicity potential of THMPP against the growth of breast cancer cells were analyzed using MTT assay (Mosmann, 1983). The cell density of 1.2×10^4 cells/well were plated in 96 well plates and maintained at 37 °C overnight. Cells were treated with varying concentrations of the samples (10, 25, 50, 75 and 100 μM) for 24 h, followed by the addition of 100 μl medium with 10 μl of MTT (5 mg/ml). As a comparative study, MDAMB-231 cells were also treated with 10 μM concentration of THMPP. H9C2, non-tumorous cells were used as a control cell line and treated with the lower concentration of 10 μM and higher concentration of 100 μM THMPP. The medium was discarded after 4 h of treatment and the formazan crystals was dissolved using 100 μl of DMSO. The purple color developed was read using microtiter plate reader at 570 nm. Cyclophosphamide was used as the positive control and the cells with the medium (untreated) serves as a control. Cell viability was calculated using the following formula:

$$\text{Viability}\ \% = \left(\frac{\text{Test OD}}{\text{Control OD}}\right) \times 100;\ \text{Cytotoxicity}\ \% = 100 - \text{Viability}\%.$$

2.3. Caspases 3 and 9 activity

Caspase-3 and -9 activities were measured by colorimetric assay kit, following the manufacturer's protocol (Calbiochem, Merck). Treated cells were lysed using the buffer containing 50 mM HEPES, 100 mM NaCl, 0.1% CHAPS, 1 mM DTT, 100 mM EDTA and centrifuged at 10000 rpm for 1 min. The extracts were carefully collected, and the protein concentration was estimated by Bradford's assay. Approximately, 100–200 μg of protein for each assay was prepared by lysing the cell with 50 μl cell lysis buffer and incubated in 96-well plates with 5 μl of the 4 mM p-nitroanilide (pNA) substrates, DEVD-pNA for 2 h at 37 °C. The Caspase-3 and -9 activities were analysed by measuring the cleaved substrate to free pNA at 405 nm in a microplate reader. The relative level of Caspase-3 and -9 were quantified using the ratio of the absorbance of THMPP treated to untreated cells.

2.4. DNA fragmentation

To study the effect of the compound in apoptosis induction in breast cancer cells, DNA of MCF-7 cells were subjected to electrophoresis. Briefly, MCF-7 cells were lysed using 100 μl of cell lysis buffer for one hour at room temperature, and the cell debris was removed by centrifugation for 15 min at 3000 rpm at 4° C. The supernatant was then mixed with equal volume of phenol: chloroform: isoamyl alcohol mixture, and then centrifuged at 5000 rpm for 15 min. The DNA was precipitated on adding 40 μl of 3.5 M ammonium acetate and ice-cold isopropanol to the aqueous phase and incubated at −20 °C for 1 h. The sample was centrifuged at 10000 rpm for 15 min and the pellet was washed with 70% ethanol and stored in 20–50 μl of TE buffer. DNA samples were electrophoresed at 50 V in 2% agarose gel (w/v). DNA was detected using EtBr staining under UV light along with DNA ladder (1 kb) as control (Basnakian and James, 1994).

2.5. RNA extraction and CDNA synthesis

Total cellular RNA from both the untreated and treated MCF-7 cells were extracted using ONE STEP-RNA Reagent (Bio Basic Canada Inc.). This method is an improved version of single-step RNA isolation using phenol and guanidine isothiocyanate (Chomzynski and Sacchi, 1987). RNA pellet was extracted and vacuum dried for 5–10 min, dissolved in DEPC treated water and stored at −20 °C. The isolated RNA (1–2 μg) was immediately reverse transcribed using EasyScript Plus™ Reverse Transcriptase primed using oligo-dT. The reaction mixture consists of 1–2 μg of RNA, 2 μl oligo-dT (stock 10 μM), with the total volume of 12.5 μl with DEPC-treated water. The mixture was incubated at 65 °C for 5 min and 1X reverse transcriptase buffer, 2.5 mM of dNTP mix, and 40 U/μl of RNase inhibitor were added in specified order. Finally, 1 μl of Easy Script reverse transcriptase (200 U/μl) was added after 5 min of incubation at 42 °C. The final reaction was set up at 42 °C for 50 min, heated up to 70 °C for 10 min and chilled on ice (Chomzynski and Sacchi, 1987).

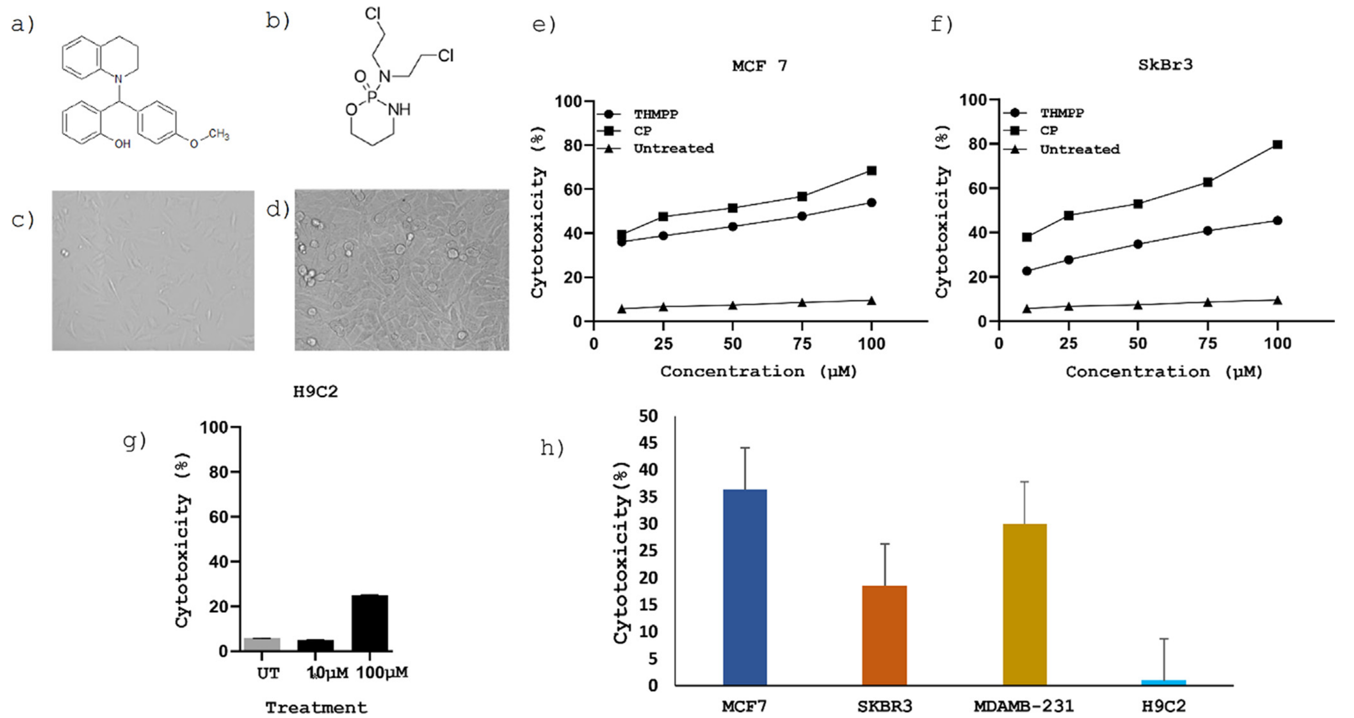

Fig. 1. Cytotoxicity effect of THMPP in different breast cancer cell lines. (a) and (b)- Ligand structure: 2D structure of THMPP and CP. IUPAC: – 2-((1, 2, 3, 4-Tetrahydroquinolin-1-yl) (4 methoxyphenyl) methyl) phenol and N,N-bis(2-chloroethyl)-2-oxo-1,3,2λ^5-oxazaphosphinan-2-amine, respectively; M. wt – 329.443 and 261.083. The phase contrast microscopic images of MCF-7 cell line (c) untreated and (d) treated. Cell cytotoxicity of THMPP in different cell lines by MTT assay (e) MCF-7 cells (f) SkBr3 cells at different concentration (10 µM, 25 µM, 50 µM, 75 µM and 100 µM) and (g) Treatment of H9C2 cells with10µM and 100 µM of THMPP. Cyclophosphamide was used as a positive control; (h) Percentage of growth inhibition in multiple breast cancer cell lines and non-tumorous cells treated with 10 µM THMPP. Data points and error bars represent mean ± S.E.M (n = 3 per group). Statistical significance was assumed for p-values *P < 0.0001.

2.6. Reverse transcription polymerase chain reaction (RT-PCR) analysis

Amplification of the target genes *EGFR*, *PI3K*, *S6K1* and β-actin were achieved using specific forward and reverse primers. β- actin, that shows the constitutive expression was used as a control for the gene expression analysis. The primers for the target mRNA were used as follows: *EGFR*, Fw: 5′- TCCCCGTAATTATGTGGT GACA GATC-3′ and Rv: 5′-ACCCCTAAATGCCACCGGC-3′ with the amplicon size 250 bp; *PI3K*, Fw: 5′-AACACAGAAGACCAATACTC-3′ and Rv: 5′-TTCGCCATCTACCACTAC-3′ with the amplicon size of 195 bp; *S6K1*, Fw: 5′-CACATAACCTGTGGTCTGTTGCTG-3′ and Rv: 5′- AGA TGCA AAGCGAACTTGGGATA-3′ with the amplicon size of 180 bp; and for reference gene *β- actin*, Fw: 5′-CACCCGCGAGTACAACCTT-3′ and Rv: 5′-CCCATACCCACCATCACACC-3′ with the amplicon size of 204 bp, were synthesized and used further for PCR reactions.

The PCR reaction was setup using the following reagents: 1X Taq Buffer (with $MgCl_2$), 0.2 mM dNTPs, 2.5 mM $MgCl_2$, 0.3 µM forward and reverse primer, template cDNA (10% of the reaction) and 1U Taq Polymerase. Amplification was performed with the following PCR conditions: initial denaturation at 94° C for 2 min and 32 cycles of 94° C for 30 s, T_a for 1 min, 72° C for 1 min 20 s with the final extension at 72° C for 7 min. T_a was specifically optimized for each gene such as 56° C for *EGFR*, 54° C for *PI3K*, 56° C for *S6K1* and 54° C for β- actin. The amplicons were separated on 1.5% agarose gel with 100 bp ladder was as a marker at 50 V for 90 min. Image J software was used to quantify the band intensity.

2.7. FACS analysis

FACS analysis was performed to check the apoptotic induction in MCF-7 cells after treatment with THMPP using FITC Annexin V (Vermes et al., 1995). FITC Annexin V stained cells negative to propidium iodide (PI) represents apoptotic cells, FITC Annexin V/PI stained cells represents late apoptosis/ necrotic cells, whereas FITC Annexin V/PI negative cells represents live cells (Koopman et al., 1994). MCF-7 cells (1 × 10^5 cells/sample) were treated with the IC_{50} concentration of THMPP and 5 µl of FITC Annexin V and 5 µl PI were added and then incubated for 15 min at 25° C in the dark. Binding buffer (1X) was added to each sample and subjected to flow cytometry analysis. The cells were acquired and gated by FITC-A and PE-A. All the measurements were performed within 1 h under similar settings in the equipment.

2.8. ACRIDINE orange/ethidium bromide (AO/ETBR) staining

Apoptosis induction by THMPP in MCF-7 was identified by AO/EtBr dual staining. As explained previously, MCF-7 cells were treated with varying concentrations of THMPP, 78.23 µM, 83.23 µM and 88.23 µM with the control well left untreated. The cells were incubated for 24 h and trypsinised. It was centrifuged, and the pellet was suspended in PBS. To 25 µl of the supernatant solution, 25 µl of staining solution containing 1:1 mixture of 100 µg/ml AO and 100 µg/ml EB was added. The cell suspension (10 µl) was observed under fluorescent microscope using blue (420–495 nm) and green filter (510–560 nm) and at least 300 cells/well was used for quantification in different fields (Basikc et al., 2006; Chowdhury et al., 2012).

2.9. Molecular docking using gold

Automated docking for THMPP against EGFR was performed using the genetic algorithm GOLD (Version 3.2 CCDC, Cambridge, UK) (Jones et al., 1997b). It has been validated earlier with a data set containing 300 protein-ligand complexes retrieved from PDB (Manikandan and Malik, 2008). To explore the ligand conformation and rotational flexibility of selected receptor, GOLD program makes use of genetic algorithm (GA). Grid box not exceeding 10 Å in size was chosen and the coordinates of the enclosing box (x = 121 Å; y = 87 Å; z = 45 Å) were also described from the active residues. Maximum of 10 different structural conformations for docking was examined and the highest binding conformers were selected for further analysis (Nissink et al., 2002).

2.10. QSAR analysis of THMPP

A quantitative structure-biological activity-property relationship (QSAR) approach was performed to quantitatively depict and provide mechanistic insights into interactions between the chemical structures of THMPP by considering the compounds with similar structures. QSAR is used for testing the relationship between the molecular descriptors of the set of compounds of interest with their respective biological activity (Roy et al., 2015). Here, 32 compounds were selected which share a significant structural similarity with the THMPP. In addition, biological activity in terms of IC_{50} were also collected from the literature (Table 1). The Dragon software calculates the descriptors for the compounds, which has about 1497 descriptors, that are classified into 18 groups. Each molecule in the training set were found to have set of 18 descriptors (Todeschini and Gramatica, 1997). Set of descriptors that are most appropriate to the IC_{50} of the compounds were selected for further analysis, and the MLR models were built and QSAR equations eliminating the variables were established using BUILDQSAR software.

2.11. ADMET analysis

The various pharmacokinetics properties and physiochemical properties of the compound, THMPP were calculated using ADMET descriptors. ADMET can provide metabolic interactions of the drug by profiling its Absorption, Distribution, Metabolism, Excretion and Toxicity properties. The prediction will contain the following important ADMET descriptors such as Blood-Brain Barrier penetration, Human Intestinal Absorption, CYP450 2C9, Caco-2 cell permeability and Ames test. The drug likeliness score of the compound determines the potentiality of the compound.

3. Results

3.1. THMPP induced cytotoxicity effect

To evaluate the effect of THMPP against the human breast cancer cell lines MCF-7 and SkBr3 and the non-cancerous mouse myoblast cells H9C2, the percentage of cell proliferation/cell viability was measured using MTT assay. The phase contrast microscopic images of the treated and untreated MCF-7 cells are represented in Fig. 1c and d. THMPP showed a dose-dependent increase in the cytotoxicity against MCF-7 cells and SkBr3 (Fig. 1e and f). The toxicity of THMPP against MCF-7 and SkBr3 cells was found to be 36.47%, 53.98% and 18.86%, 40.47% at 10 μM and 100 μM, respectively. The IC_{50} concentration of THMPP against was less in MCF-7 with 83.23 μM than SkB3 cells with 113.94 μM (Fig. 1e and f). Cyclophosphamide was used as a positive control, where its cytotoxicity against MCF-7 and SkBr3 was significantly high. The IC_{50} value of CP against MCF-7 and SkBr3 was found to be 42.79 μM and 38.34 μM, respectively (Fig. 1e and f). Also, THMPP

Table 1
List of training set and test set compounds with its IC_{50} values.

S.No	Compound Name	IC_{50}	References
Training Set			
1	2-((1,2,3,4-tetrahydroquinolin-1-yl)(4-methoxyphenyl)methyl)phenol	83.23	Present Study
2	Curcusone B	0.2	Sawadogo et al., 2012
3	Curcusone C	0.08	
4	Curcusone D	0.1	
5	voruscarin	4	
6	Uscharin	4	
7	2-Hydroxy-isojatrogrossidion	0.2	
8	2-epi-hydroxyisojatrogrossidion	0.2	
9	Multidione	5.5	
10	4Z jatrogrossidentadion	0.6	
11	4E jatrogrossidentadion	2.1	
12	Pinostrobin	10.2	
13	Balanitin-6/7	2.6	
14	Jatropholone	7.5	
15	Multi-substituent phenyl derivatives 1	1.38	Tao et al., 2010
16	Multi-substituent phenyl derivatives 4	11.74	
17	Mangrove-derived quinones 7	0.17	
18	Mangrove-derived quinones 8	2.53	
19	Mangrove-derived quinones 9	1.43	
20	Mangrove-derived quinones 11	13.23	
21	Mangrove-derived quinones 13	16.32	
Test Set			
S.No	Compound Name	IC_{50}	References
1	Mangrove-derived quinones 14	35.23	Tao et al., 2010
2	Mangrove-derived quinones 18	17.22	
3	Isoflavone analog 78	19.77	
4	Fatty acid derivatives 81	0.41	
5	Phytol	34	Malek et al., 2008
6	phenolic constituents 4	62.9	El Molla et al., 2016
7	phenolic constituents 6	63.8	

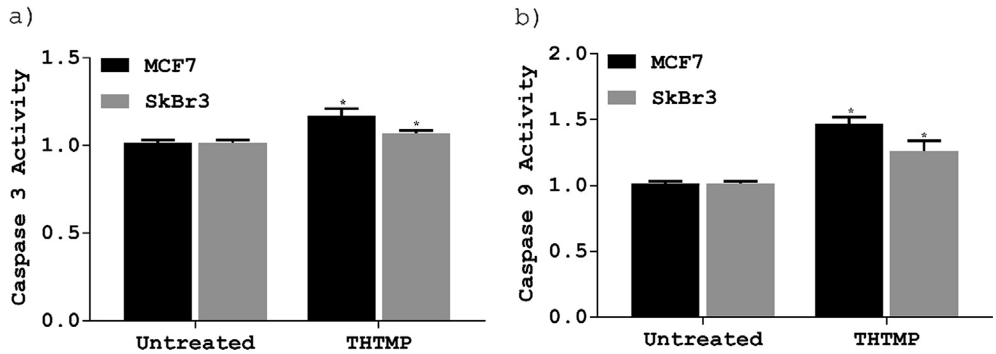

Fig. 2. Caspase-3 and Caspase-9 activity in THMPP treated MCF-7 and SkBr3 cell lines. (a) Relative caspase-3 activity of THMPP treated MCF-7 and SkBr3 compared with the untreated cells. The results were considered significant (two way ANOVA) in comparison with the untreated group (*, $P \leq 0.007$). (b) Relative caspase-9 activity of THMPP treated MCF-7 and SkBr3 compared with the untreated cells. The results were considered significant (two way ANOVA) in comparison with the untreated group (*, $P < 0.0001$). Data represents Mean ± SEM (n = 3 experiment).

has least percentage of cytotoxicity to non-cancerous cells, H9C2 (0.91%) when compared with other breast cancer cell lines such as MCF-7(36%), SkBr3(18%) and MDAMB-231(30%) upon treatment with 10 μM of THMPP (Fig. 1g and h). These results suggested that THMPP has the ability to specifically target breast cancer cell lines than the normal cells. The differences in the treated conditions was found to be statistically significant as per two-way ANOVA (P-value < 0.0001).

3.2. Caspase-3 and caspase-9 induction

To clarify whether THMPP could induce apoptosis, caspase-3 and -9 activities were measured in MCF-7 and SkBr3. The cells were treated with the respective IC_{50} concentration of THMPP. In both the cell lines, there was significant fold change in the enzyme activity after the treatment. In MCF-7 cells, it was found that the caspase-3 and -9 activities were increased by a fold level of 0.17 and 0.47, whereas in SkBr3, fold change of 0.07 and 0.25 was observed respectively, when compared to the untreated cells (Fig. 2a and b). Thus, THMPP could activate caspase enzyme activity, thereby induces apoptosis in both the cell lines. The values were statistically significant, as per two-way ANOVA test (P < 0.0001).

3.3. Induction of DNA strand break by THMPP

To further substantiate the ability of THMPP in inducing apoptosis, the cells were subjected for DNA fragmentation assay. The DNA fragmentation is a sign of apoptosis, which causes nicks in genomic DNA of the cells (Eastman and Barry, 1992). The genomic DNA from THMPP treated MCF-7 cells was isolated and analysed by agarose gel electrophoresis. The result shows that untreated cells have intact DNA with no laddering whereas treated cells showed a characteristic ladder of inter-nucleosomal fragmentation, confirming the induction of apoptosis (Fig. 3a).

3.4. Analysis of apoptosis induction by THMPP using Annexin V/PI

The phosphatidylserine externalization in MCF-7 cells stained with Annexin V-FITC/PI was quantified by flow cytometry to assess the apoptotic cell death. The analysis showed that THMPP could induce apoptosis in a concentration-dependent manner (Fig. 3). The untreated cells were mostly viable. The cells with compromised membrane were analysed by staining using membrane impermeable dye, PI. Thus the counter staining with PI and Annexin V delineates the cells at different cell phase. The cells treated with THMPP showed 3.21% of early apoptotic cells, 36.02% of late apoptotic cells and 59.7% viable cells (Fig. 3d). This substantiates the effect of THMPP in apoptosis mediated cell death (Fig. 3b and c).

MCF-7 cells were treated with a varying doses of THMPP for 24 h, as described in the method section. Apoptotic cell death causing nuclear fragmentation was assessed upon treatment with varying concentration of THMPP and the cells were observed under flourescent microscope (Fig. 4). The dual AO/EB fluorescent staining qualitatively and quantitatively reveals the morphological

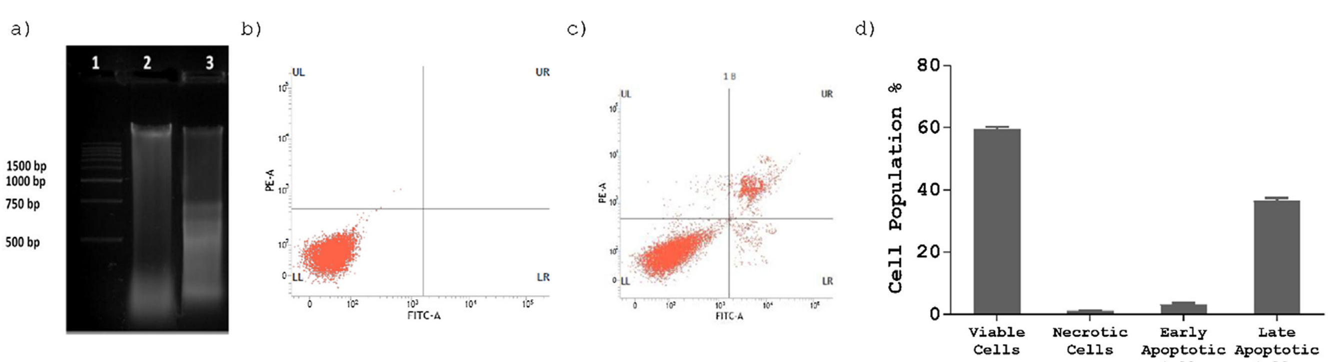

Fig. 3. DNA fragmentation of MCF-7 cells exposed to THMPP (a) DNA gel electrophoresis of internucleosomal DNA fragmentation in 1.5% Agarose gel upon treatment with THMPP in MCF-7 cell lines (lane 1) Marker-1 Kb ladder; (lane 2) negative control without treatment; (lane 3) DNA of cells treated with THMPP. Assessment of apoptosis by FACS of apoptosis in THMPP (IC_{50} – 83.23 μM) treated MCF-7 cells measured using FITC-labelled annexin V/PI (b) untreated cells; (c) THMPP treated MCF-7 cells. UL- necrotic cells, UR- late apoptotic cells, LL - viable cells, LR – early apoptotic cells. (d) Quantitative analysis on the percentage of viable, apoptotic, or necrotic cells by FACS analysis.

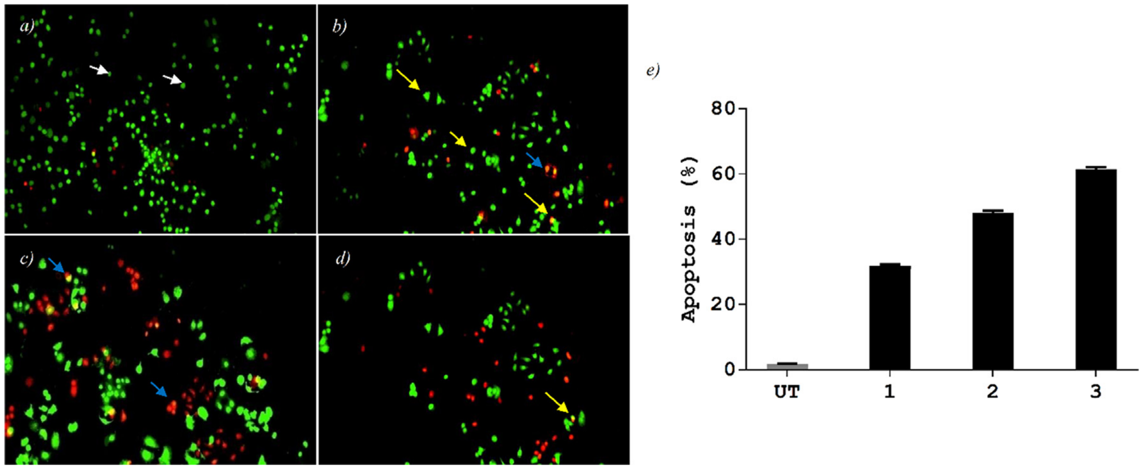

Fig. 4. Fluorescence microscopy images of AO-EtBr stained MCF-7 cells after treatment with THMPP. (a) Untreated cells; MCF-7 cells treated with THMPP at different concentrations (b) 78.23 μM, (c) 83.23 μM and (d) 88.23 μM. The white, yellow and blue arrows are representing viable, early apoptotic, and late apoptotic cells respectively. (e) percentage of apoptosis at different concentrations, where treatment 1 is 78.23 μM; treatment 2 is 83.23 μM; and treatment 3 is 88.23 μM.

changes in apoptotic cells, with clear distinction between normal cells, apoptotic cells, and necrotic cells.

The Fig. 4a–d showed the mode of cell death by dual AO/EB staining. Control cells (untreated MCF-7 cells) are normal healthy cells with green fluorescent cells having normal cytoplasm and nuclei morphology, and represents only less than 2% cells in apoptotic stage. The cells entering early apoptosis appears yellowish green fluorescence with membrane blebbing and those cells in late apoptosis appeared orange/red fluorescence. It is observed that 48% of the cells were in apoptotic stage upon treatment with 83.23 μM of THMPP, 61% cells at 88.23 μM and 32% cells at 78.23 μM of THMPP treatment. As the concentration of the compound increases, there is a significant increase in the apoptosis induction and thus THMPP induces cell death through apoptosis pathway (Fig. 4e).

3.5. Effect of THMPP on the expression of PI3K and S6K1 genes

To further understand the mechanism of action of THMPP, we examined the influence of THMPP in PI3K signaling pathway.

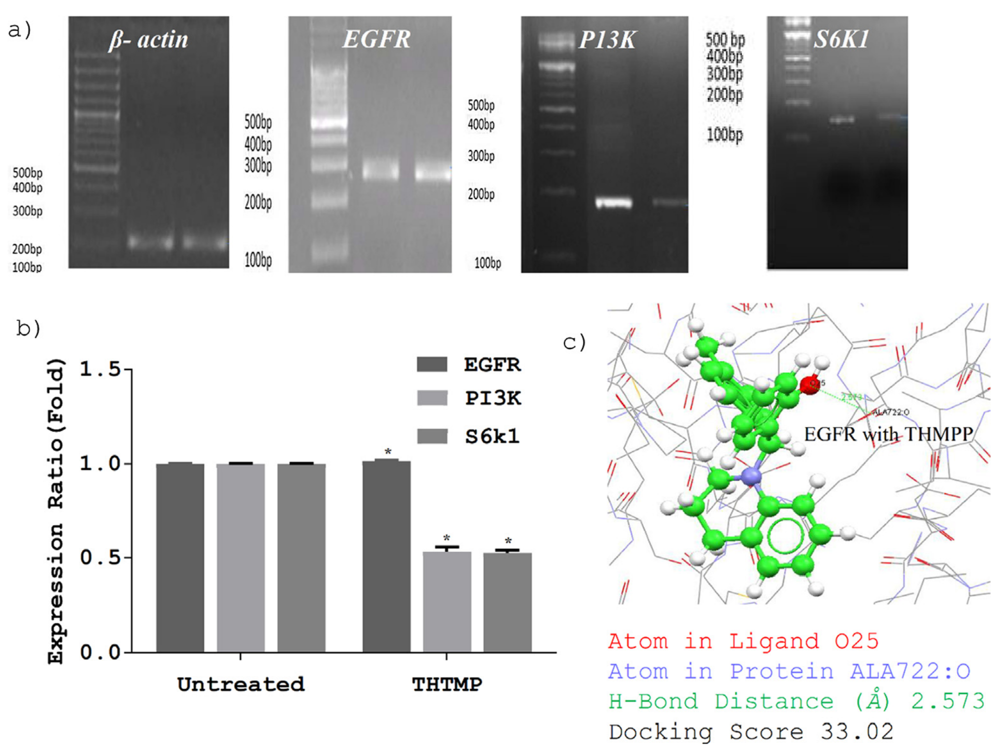

Fig. 5. Gene expression analysis in MCF-7 cell upon THMPP treatment. (a) RT-PCR amplification of *β- actin* (204 bp), *EGFR* (250 bp), *P13K* (195 bp) and *S6K1* genes (180 bp). (Lane 1: 100 bp DNA marker, Lane 2: control (untreated) Lane 3: (PCR amplicon treated with THMPP); (b) Optical density was measured to evaluate the mRNA expression of *EGFR; S6K1; PI3K*, with the housekeeping gene *β-actin* serving as the normalization control. The fold change represented as the expression ratio of the genes. Data points and error bars represent mean ± S.E.M (n = 3 per group). Statistical significance was assumed for p-values *P < 0.0001. (c) Molecular docking analysis of THMPP with EGFR. The surface-docking model of THMPP in the EGFR active site. The ligand is represented as sticks; and the protein active sites as lines, hydrogen bond interaction are shown in dotted lines (Red) and the interacting residues are labelled.

Semi-quantitative RT-PCR was carried out using primers specific for *EGFR, PI3K and S6K1* genes with β-actin as the reference control. The genes with respective band size of 204 bp (β-*actin*), 250 bp (*EGFR*), 195 bp (*PI3K*) and 180 bp (*S6K1*) were observed clearly in agarose gel (Fig. 5a). The ImageJ was used to calculate the expression fold of each gene. EGFR gene expression was not altered upon THMPP treatment when compared with the untreated cell lines. But, there occurs a reduced level of altered gene expression level with 0.5 fold change in both *PI3K* and *S6K1* (Fig. 5b). These results suggest that the THMPP could induce apoptosis by down regulating the expression of genes, *PI3K* and *S6KI* involved in PI3K/AKT signalling pathway (Fig. 5b). The values were found to be statistically significant, as per two way ANOVA test (P-value < 0.0001).

3.6. Molecular docking of THMPP with EGFR

Molecular docking was performed using GOLD (Jones et al., 1997b). The 3D structure of EGFR was availed from protein data bank with the PDB ids: 2RGP. Binding compatibility was evaluated based on the docked energy in kcal/mol (Fig. 5c). The active sites present in the crystal structure of the five receptors were obtained from the pdbsum database which was further used for the docking analysis. The following amino acids are present in the 32 active sites of EGFR receptors, ie., Leu718, Gly719, Ala722, Val726, Ala743, Lys745, Met766, Cys775, Arg776, Leu777, Leu788, Thr790, Gln791, Leu792, Met793, Pro794, Phe795, Gly796, Asp800, Arg803, Arg832, Leu833, Val834, His835, Arg836, Asp837, Leu844, Leu862, His888, Lys913, Lys970, Arg977. Many significant interactions were predicted between the ligand (THMPP) and the receptor (EGFR). The best docking score of 33.02 determines the best interaction. The Fig. 5c represents the docking score and residual values of the interaction.

3.7. THMPP structure activity relationship and its pharmacokinetics properties

BUILDQSAR was used to predict the anti-cancer potential of the compound, THMPP. Based on the compounds selected (Table 1), a QSAR model was built. The regression line was plotted and the compounds that significantly deviate away were considered as outliers and excluded from the modelling procedure. The QSAR model was tested against the compounds in the test set and the predictability of the QSAR model was validated (Fig. 6) using the correlation coefficient value, (r) 0.970 for training set (Fig. 6a) and 0.985 for the test set (Fig. 6b). This shows the efficiency of the model generated and the results clearly indicated that the compound was predicted to be a potent anti-cancer agent. In particular, THMPP correlates well with the equation, which substantiates its toxic effect against cancer cells.

Table 2
ADME and drug likeness properties of the ligand THMPP.

End Points	HTS Data	Accuracy
Blood-Brain Barrier	BBB+	0,8003
Human Intestinal Absorption	HIA+	0,9971
Caco-2 Permeability	Caco2+	0,5375
P-glycoprotein Substrate	Non-substrate	0,7583
P-glycoprotein Inhibitor	Non-inhibitor	0,6068
	Non-inhibitor	0,9278
Renal Organic Cation Transporter	Non-inhibitor	0,8148
Subcellular localization	Mitochondria	0,6819
CYP450 2C9 Substrate	Non-substrate	0,6246
CYP450 2D6 Substrate	Non-substrate	0,8092
CYP450 3A4 Substrate	Substrate	0,6311
CYP450 1A2 Inhibitor	Inhibitor	0,7358
CYP450 2C9 Inhibitor	Inhibitor	0,651
CYP450 2D6 Inhibitor	Non-inhibitor	0,8645
CYP450 2C19 Inhibitor	Non-inhibitor	0,5508
CYP450 3A4 Inhibitor	Non-inhibitor	0,7413
CYP Inhibitory Promiscuity	High CYP Inhibitory Promiscuity	0,7253
Human Ether-a-go-go-Related Gene Inhibition	Strong inhibitor	0,5167
	Non-inhibitor	0,7336
AMES Toxicity	AMES toxic	0,9402
Carcinogens	Non-carcinogens	0,6772
Fish Toxicity	High FHMT	0,9583
Tetrahymena Pyriformis Toxicity	High TPT	0,9846
Honey Bee Toxicity	Low HBT	0,513
Biodegradation	Not ready biodegradable	0,9604
Acute Oral Toxicity	Category III	0,7048
Carcinogenicity (Three-class)	Warning	0,4551

Further, the results of the ADMET analysis are shown in the Table 2. The oral bioavailability and ADMET risk profiling were within their acceptable limit for THMPP. It obeyed Lipinski rule of five and had good absorption properties. Also, it is predicted to cross the Blood Brain Barrier and has Caco-2 permeability and good intestinal absorption and predicted to be localized in mitochondria of the cell. The metabolism and toxicity parameters are also acceptable for THMPP. The complete endpoints prediction concludes that the compound THMPP, exhibits good drug likeliness properties.

4. Discussion

Several studies are reported on various natural and synthetic phenolics to have cytotoxic effect on cancer cells. (Liu et al., 2018; LS et al., 2016; Spatafora and Tringali, 2012). Reports on

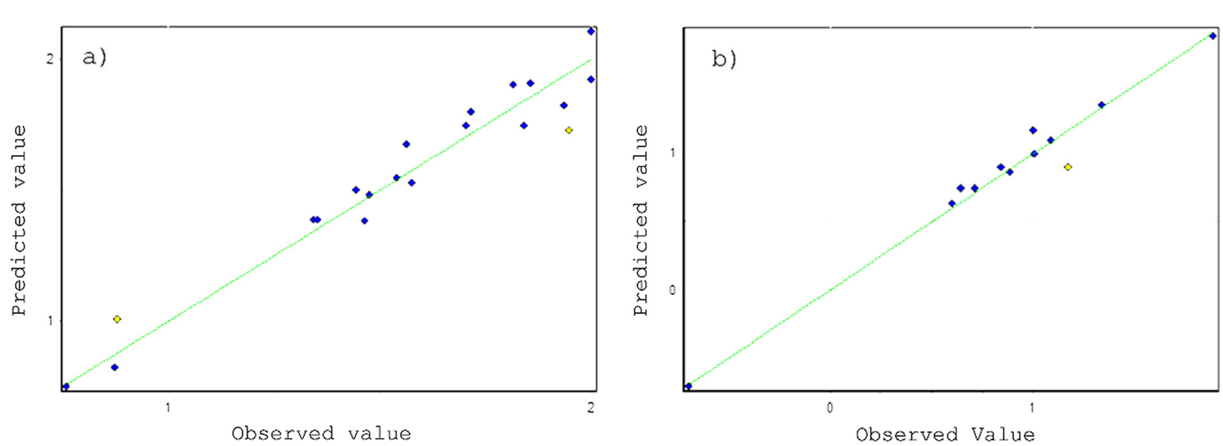

Fig. 6. QSAR Correlation plot. (a) Training set correlation coefficient (R2 = 0.970). (b) Test set correlation coefficient (R2 = 0.985).

phenolic derivative like phenolic acids are available which deal with anti-oxidant property and their action on cancer cell proliferation. Many dietry phenolic acids have also been tested. In particular, the well known phenolics, caffeic acid when treated with breast cancer cells, T47D showed good growth inhibition with the IC_{50} of 2.17×10^{-9} M (Kampa et al., 2004b). Phenolic compounds which are structurally related have been also shown to induce cell cycle arrest and apoptosis of cancer cells(Ahmad et al., 2011) (Amawi et al., 2017).

The susceptible nature of tumor cells to apoptosis is the vital determinant of chemotherapy efficacy (Stumm et al., 2004). Thus, an effective anti-cancer drugs, which can target breast cancer cells by inducing apoptosis is needed for efficient treatment. We determined the ability of THMPP to induce apoptosis in breast cancer cells using DNA fragmentation analysis, Caspase3/9 activity assay, FITC/Annexin staining and AO/EtBr fluorescent staining procedures. It is evident that, THMPP induced apoptosis via caspase 3/9 activation, but then other signaling pathways might also be induced along with caspase 3/9 activation. Therefore, further analysis of apoptosis and/or autophagy signaling pathway on multiple cancer cell types should be implemented for anticancer development.

On the other hand, expression of genes involved in the tumor progression is altered in cancer conditions. PI3K/AKT/S6K1/mTOR pathway promotes cell survival and cell proliferation, which is continuously over-expressed in breast cancer cells. In this study, the newly synthesized THMPP was able to down regulate *PI3K* and *S6K1* genes, which could suppress proliferation and induce apoptosis. Also, decrease in the *S6K1* expression reduces the risk of radiation resistance of cancer cells(Tandon et al., 2011). This attribute reduces the risk of side effects which are common in chemotherapeutic agents. Similar researches were also carried out in the well known polyphenols of green and black tea and were reported to have anti-cancer properties by up- or down-regulating a number of key enzymes (Beltz et al., 2006). Overall, THMPP was identified to be a candidate drug to treat multiple breast cancer and further clinical trials in animal model is essential to verify the antitumor activity.

5. Conclusion

The present investigation revealed that THMPP can act as a potential drug for treating breast cancer. This study demonstrated that THMPP has cytotoxic activity on MCF-7 and SkBr3 breast cancer cell line. THMPP was determined to be apoptosis induced, triggering DNA fragmentation as well as caspase 3/9 in human breast cancer cell lines. Additionally, molecular docking of THMPP with EGFR identified that the can potentially interact with EGFR and activate its downstream signaling pathway. Gene expression analysis also confirms the downregulation of *PI3K*, suggesting that THMPP might de-regulate the EGFR signaling pathway in breast cancer cells. The QSAR and ADMET analysis also proves that THMPP as non carcinogenic and a good drug-like candidate for breast cancer treatment. Overall, we anticipate that THMPP can be technically exploited further for the development of an effective anti-breast cancer agents.

Author contributions

SP executed the experiments and data analysis. AK involved in technical discussion and management. OY and MK conceived and managed all studies. All the authors contributed to writing the manuscript.

Ethical approval

This article does not contain any studies with human participants performed by any of the authors.

Acknowledgement

We would like to thank Prof. Nuno R. Candeias, Faculty of Engineering and Natural Sciences, Tampere University for gift of synthesized compounds.

Declaration of Competing Interest

The authors declare that they have no known competing financial interests or personal relationships that could have appeared to influence the work reported in this paper.

References

Ahmad, A., Sakr, W.A., Rahman, K.W., 2011. Mechanisms and therapeutic implications of cell death induction by indole compounds. Cancers (Basel) 3, 2955. https://doi.org/10.3390/CANCERS3032955.

Amawi, H., Ashby, C.R., Samuel, T., Peraman, R., Tiwari, A.K., Tiwari, A.K., 2017. Polyphenolic nutrients in cancer chemoprevention and metastasis: role of the epithelial-to-mesenchymal (EMT) pathway. Nutrients 9. https://doi.org/10.3390/nu9080911.

Basikc, D., Papovic, S., Ristic, P., Arsenijevic, N., 2006. Analysis of cycloheximide-induced apoptosis in human leukocytes: fluorescence microscopy using annexin V/propidium iodide versus acridin orange/ethidium bromide. Cell Biol. Int. 30, 924–932. https://doi.org/10.1016/j.cellbi.2006.06.016.

Basnakian, A.G., James, S.J., 1994. A rapid and sensitive assay for the detection of DNA fragmentation during early phases of apoptosis. Nucleic Acids Res. 22, 2714–2715.

Beltz, L.A., Bayer, D.K., Moss, A.L., Simet, I.M., 2006. Mechanisms of cancer prevention by green and black tea polyphenols. Anticancer. Agents Med. Chem. 6, 389–406.

Bray, F., Ferlay, J., Soerjomataram, I., Siegel, R.L., Torre, L.A., Jemal, A., 2018. Global cancer statistics 2018: GLOBOCAN estimates of incidence and mortality worldwide for 36 cancers in 185 countries. CA Cancer J. Clin. 68, 394–424. https://doi.org/10.3322/caac.21492.

Chomzynski, P., Sacchi, N., 1987. Single-step method of RNA isolation by acid guanidinium thiocyanate–phenol–chloroform extraction. Anal. Biochem. 162, 156–159. https://doi.org/10.1006/abio.1987.9999.

Chowdhury, S., Kandhavelu, M., Yli-Harja, O., Ribeiro, A.S., 2012. An interacting multiple model filter-based autofocus strategy for confocal time-lapse microscopy. J. Microsc. https://doi.org/10.1111/j.1365-2818.2011.03568.x.

Ciruelos Gil, E.M., 2014. Targeting the PI3K/AKT/mTOR pathway in estrogen receptor-positive breast cancer. Cancer Treat. Rev. 40, 862–871. https://doi.org/10.1016/j.ctrv.2014.03.004.

Doan, P., Musa, A., Candeias, N.R., Emmert-Streib, F., Yli-Harja, O., Kandhavelu, M., 2019. Alkylaminophenol induces G1/S phase cell cycle arrest in glioblastoma cells through p53 and cyclin-dependent kinase signaling pathway. Front. Pharmacol. https://doi.org/10.3389/fphar.2019.00330.

Doan, P., Nguyen, T., Yli-Harja, O., Candeias, N.R., Kandhavelu, M., 2017. Effect of alkylaminophenols on growth inhibition and apoptosis of bone cancer cells. Eur. J. Pharm. Sci. 107, 208–216. https://doi.org/10.1016/j.ejps.2017.07.016.

El Molla, S.G., Motaal, A.A., El Hefnawy, H., El Fishawy, A., 2016. Cytotoxic activity of phenolic constituents from Echinochloa crus-galli against four human cancer cell lines. Brazilian J. Pharmacogn. https://doi.org/10.1016/j.bjp.2015.07.026.

Jones, G., Willett, P., Glen, R.C., Leach, A.R., Taylor, R., 1997b. Development and validation of a genetic algorithm for flexible docking. J. Mol. Biol. https://doi.org/10.1006/jmbi.1996.0897.

Kampa, M., Alexaki, V.-I., Notas, G., Nifli, A.-P., Nistikaki, A., Hatzoglou, A., Bakogeorgou, E., Kouimtzoglou, E., Blekas, G., Boskou, D., Gravanis, A., Castanas, E., 2004b. Introduction Antiproliferative and apoptotic effects of selective phenolic acids on T47D human breast cancer cells: potential mechanisms of action. https://doi.org/10.1186/bcr752.

Karjalainen, A., Yli-Harja, O., Kandhavelu, M., Doan, P., Candeias, N.R., Sandberg, O., Chandraseelan, J.G., 2017. Synthesis of phenol-derivatives and biological screening for anticancer activity. Anticancer. Agents Med. Chem. 17, 1710–1720. https://doi.org/10.2174/1871520617666170327142027.

Kato, S., Endoh, H., Masuhiro, Y., Kitamoto, T., Uchiyama, S., Sasaki, H., Masushige, S., Gotoh, Y., Nishida, E., Kawashima, H., Metzger, D., Chambon, P., 1995. Activation of the estrogen receptor through phosphorylation by mitogen-activated protein kinase. Science 270, 1491–1494.

Koopman, G., Reutelingsperger, C.P., Kuijten, G.A., Keehnen, R.M., Pals, S.T., van Oers, M.H., 1994. Annexin V for flow cytometric detection of phosphatidylserine expression on B cells undergoing apoptosis. Blood 84, 1415–1420.

Liu, J., Ming, B., Gong, G.-H., Wang, D., Bao, G.-L., Yu, L.-J., 2018. Current research on anti-breast cancer synthetic compounds. https://doi.org/10.1039/c7ra12912b.

Ls, R., Nja, S., Ncp, S., Mc, M., Aj, T., 2016. Anticancer properties of phenolic acids in colon cancer – a review. J. Nutr. Food Sci. 06, 1–7. https://doi.org/10.4172/2155-9600.1000468.

Malek, S.N.A., Wahab, N.A., Yaacob, H., Shin, S.K., Lai, H.S., Serm, L.G., Rahman, S.N.S. A., 2008. Cytotoxic Activity of Pereskia bleo (Cactaceae) Against Selected Human Cell Lines. Int. J. Cancer Res. 4, 20–27. https://doi.org/10.3923/ijcr.2008.20.27.

Manikandan, S., Malik, B.K., 2008. Modeling of human CCR5 as target for HIV-I and virtual screening with marine therapeutic compounds. Bioinformation 3, 89–94.

Martelli, A.M., Chiarini, F., Evangelisti, C., Grimaldi, C., Ognibene, A., Manzoli, L., Billi, A.M., McCubrey, J.A., 2010. The phosphatidylinositol 3-kinase/AKT/mammalian target of rapamycin signaling network and the control of normal myelopoiesis. Histol. Histopathol. 25, 669–680. https://doi.org/10.14670/HH-25.669.

Mosmann, T., 1983. Rapid colorimetric assay for cellular growth and survival: application to proliferation and cytotoxicity assays. J. Immunol. Methods 65, 55–63.

Nissink, J.W.M., Murray, C., Hartshorn, M., Verdonk, M.L., Cole, J.C., Taylor, R., 2002. A new test set for validating predictions of protein-ligand interaction. Proteins Struct. Funct. Bioinforma. 49, 457–471. https://doi.org/10.1002/prot.10232.

Roy, K., Kar, S., Das, R.N., Roy, K., Kar, S., Das, R.N., 2015. Validation of QSAR models. Underst. Basics QSAR Appl. Pharm. Sci. Risk Assess., 231–289 https://doi.org/10.1016/B978-0-12-801505-6.00007-7.

Sawadogo, W.R., Le Douaron, G., Maciuk, A., Bories, C., Loiseau, P.M., Figadère, B., Guissou, I.P., Nacoulma, O.G., 2012. In vitro antileishmanial and antitrypanosomal activities of five medicinal plants from Burkina Faso. Parasitol. Res. 110, 1779–1783. https://doi.org/10.1007/s00436-011-2699-3.

Spatafora, C., Tringali, C., 2012. Natural-derived polyphenols as potential anticancer agents. Anticancer. Agents Med. Chem. 12, 902–918. https://doi.org/10.2174/187152012802649996.

Stumm, S., Meyer, A., Lindner, M., Bastert, G., Wallwiener, D., Gückel, B., 2004. Paclitaxel treatment of breast cancer cell lines modulates fas/fas ligand expression and induces apoptosis which can be inhibited through the CD40 receptor. Oncology 66, 101–111. https://doi.org/10.1159/000077435.

Sun, M., Paciga, J.E., Feldman, R.I., Yuan, Z., Coppola, D., Lu, Y.Y., Shelley, S.A., Nicosia, S.V., Cheng, J.Q., 2001. Phosphatidylinositol-3-OH kinase (PI3K)/AKT2, activated in breast cancer, regulates and is induced by estrogen receptor (ER) via interaction between ER and PI3K 1. Cancer Res. 61, 5985–5991.

Tandon, P., Gallo, C.A., Khatri, S., Barger, J.F., Yepiskoposyan, H., Plas, D.R., 2011. Requirement for ribosomal protein S6 kinase 1 to mediate glycolysis and apoptosis resistance induced by Pten deficiency. Proc. Natl. Acad. Sci. U.S.A. 108, 2361–2365. https://doi.org/10.1073/pnas.1013629108.

Tao, L.Y., Zhang, J.Y., Liang, Y.J., Chen, L.M., Zheng, L.S., Wang, F., Mi, Y.J., She, Z.G., To, K.K.W., Lin, Y.C., Fu, L.W., 2010. Anticancer effect and structure-activity analysis of marine products isolated from metabolites of mangrove fungi in the South China Sea. Mar. Drugs. https://doi.org/10.3390/md8041094.

Todeschini, R., Gramatica, P., 1997. 3D-modelling and Prediction by WHIM descriptors. Part 6. Application of WHIM descriptors in QSAR studies. Quant. Struct. Relationships 16, 120–125. https://doi.org/10.1002/qsar.19970160204.

Vaiyapuri, P.S., Ali, A.A., Mohammad, A.A., Kandhavelu, J., Kandhavelu, M., 2015. Time lapse microscopy observation of cellular structural changes and image analysis of drug treated cancer cells to characterize the cellular heterogeneity. Environ. Toxicol. 30, 724–734. https://doi.org/10.1002/tox.21950.

Vermes, I., Haanen, C., Steffens-Nakken, H., Reutelingsperger, C., 1995. A novel assay for apoptosis. Flow cytometric detection of phosphatidylserine expression on early apoptotic cells using fluorescein labelled Annexin V. J. Immunol. Methods 184, 39–51.